Morphology of QSOs
the gridpoints of the Gaia Celestial Reference Frame

Alexandre H. Andrei [1,2,3,4] , *Sonia Anton* [5] , *François Taris* [3] ,
Sébastien Bouquillon [3] , *Jean Souchay* [3] , *Roberto Vieira Martins* [1] ,
Júlio I. Bueno de Camargo [1] , *Marcelo Assafin* [4] , *Christophe Barache* [3] ,
Dario N. da Silva Neto [6]

(1) Observatório Nacional/MCTI-BR
(2) Osservatorio Astronomico di Torino/INAF-IT
(3) SYRTE/Observatoire de Paris-FR
(4) Observatório do Valongo/UFRJ-BR
(5) Centro de Investigação em Ciências Geo-Espaciais/FCUP and SIM – PO
(6) UEZO/RJ-BR

Abstract

The acronym QSO refers to the particular time in the life of giant galaxies, often elliptic ones, when the nucleus becomes extremely active fueled by matter infalling onto the accretion disk feeding the massive central black hole. But the duration and intensity of such a phase make QSOs to be treated as a class of objects, and indeed a class of enhanced cosmologic, astrophysical and astrometric bearings. As a consequence, even in the optical domain, the morphology of a quasar can be understood as comprehending the domineering central source, the immediate surrounding regions, the jet basis and features along the jet, and a bright host galaxy which is likely to be intensely star forming and generally speaking a lively place in itself. Morphology, and its color dependent aspects, can thus inform on the physical processes at work on a given QSO, for example what is likeness to exhibit different time scales of variability. The ESA Gaia mission will have its fundamental reference frame formed by quasars, which are desired to be as pointlike as can be gathered for the sake of ensuring maximum astrometric precision and accuracy. We will present how the morphology characteristic is indicated in the Gaia Initial QSO Catalog and the related investigations. We will also outline the Gaia extended sources methods that will be applied to all QSOs observed, and the vast amount of information that will be made available from the mission outcomes.

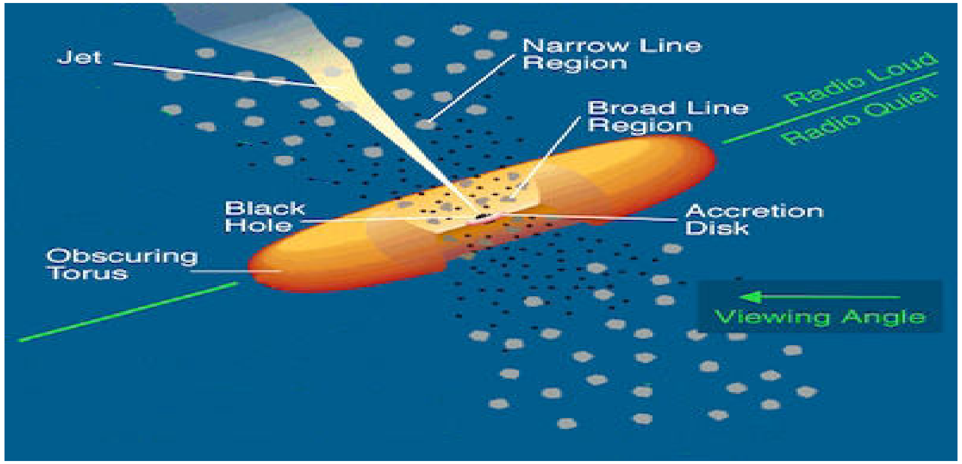
Jet
Narrow Line Region
Broad Line Region
Radio Loud
Radio Quiet
Black Hole
Accretion Disk
Obscuring Torus
Viewing Angle

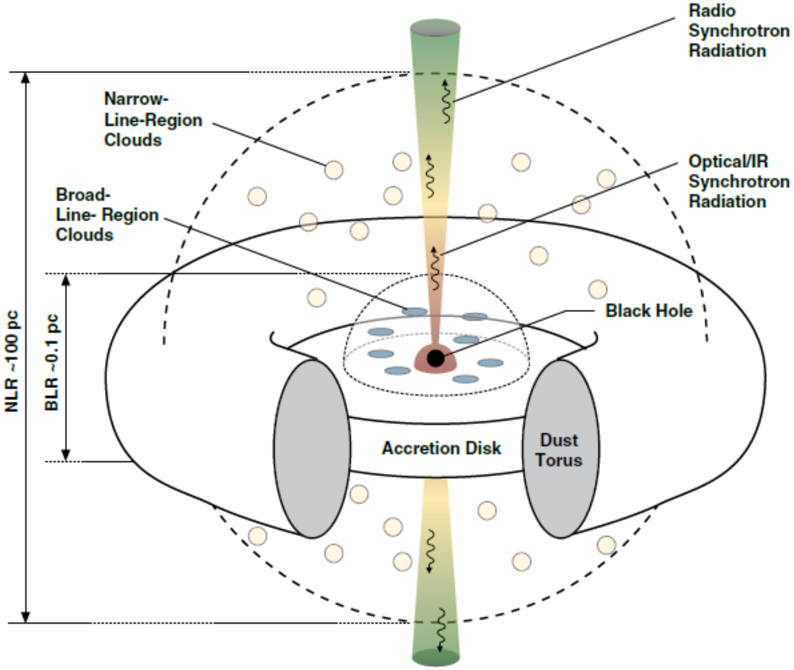
Radio Synchrotron Radiation
Narrow-Line-Region Clouds
Optical/IR Synchrotron Radiation
Broad-Line- Region Clouds
Black Hole
NLR ~100 pc
BLR ~0.1 pc
Accretion Disk
Dust Torus

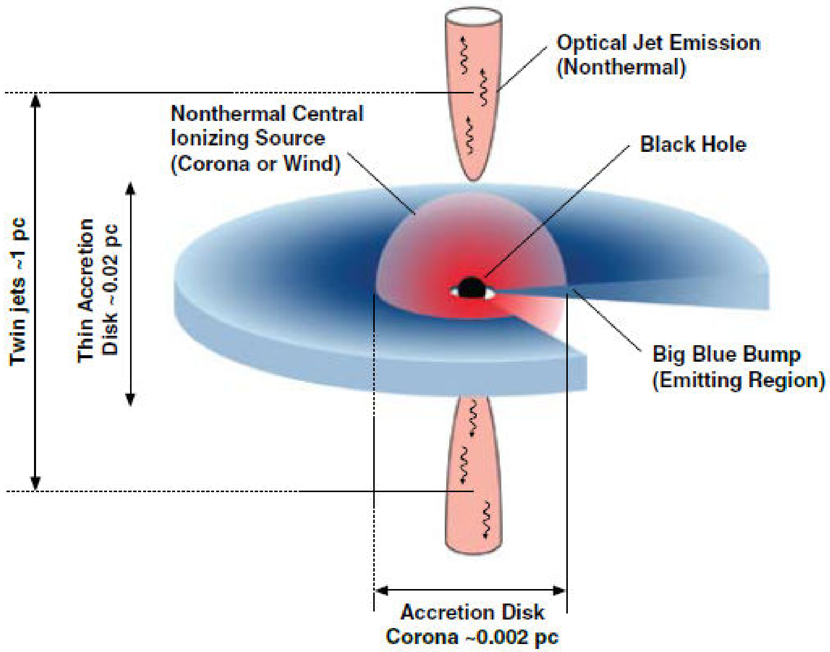
Optical Jet Emission (Nonthermal)
Nonthermal Central Ionizing Source (Corona or Wind)
Black Hole
Twin jets ~1 pc
Thin Accretion Disk ~0.02 pc
Big Blue Bump (Emitting Region)
Accretion Disk Corona ~0.002 pc

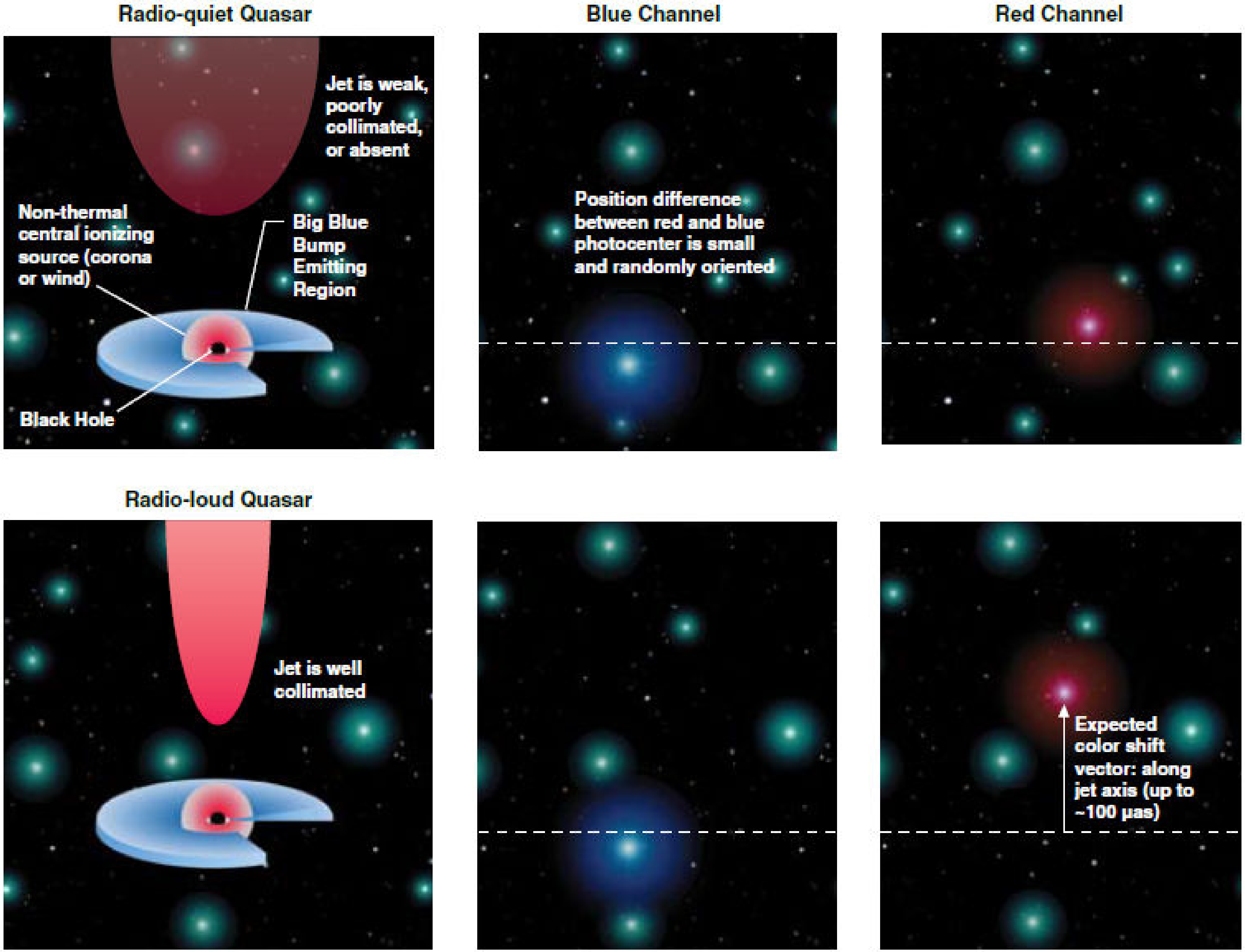
Radio-quiet Quasar
Blue Channel
Red Channel
Jet is weak, poorly collimated, or absent
Non-thermal central ionizing source (corona or wind)
Big Blue Bump Emitting Region
Black Hole
Position difference between red and blue photocenter is small and randomly oriented
Radio-loud Quasar
Jet is well collimated
Expected color shift vector: along jet axis (up to ~100 μas)

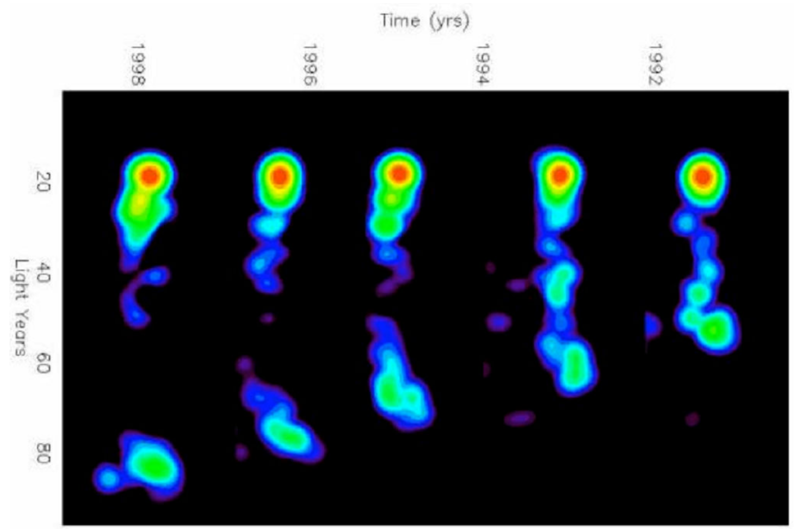
Time (yrs)
1998
1996
1994
1992
Light Years
20
40
60
80

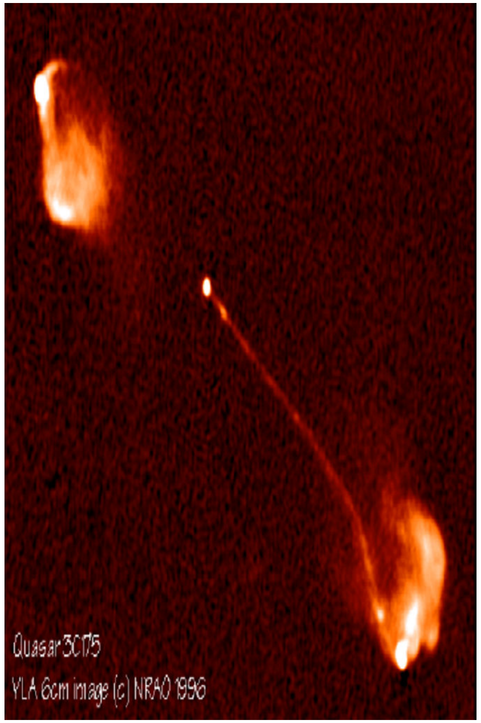
Quasar 3C175
VLA 6cm image (c) NRAO 1996

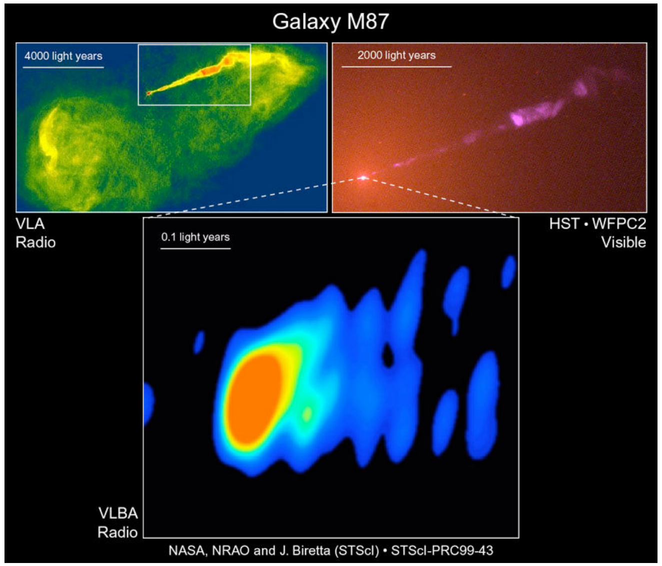
Galaxy M87
4000 light years
2000 light years
VLA
Radio
HST • WFPC2
Visible
0.1 light years
VLBA
Radio
NASA, NRAO and J. Biretta (STScI) • STScI-PRC99-43

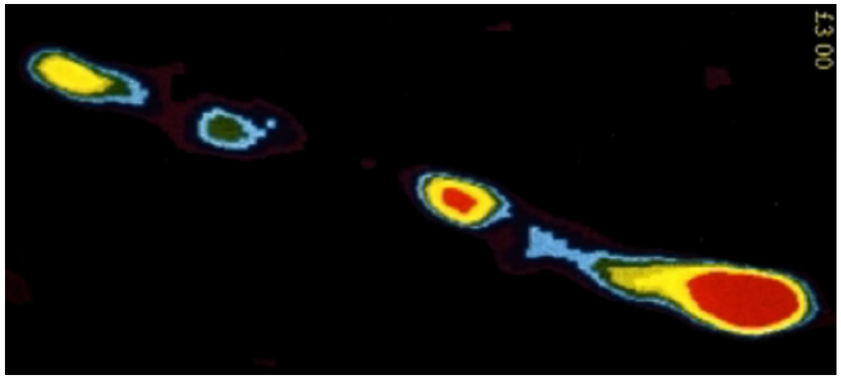

The Gaia Initial Quasar Catalog – Morphology and Variability

1) Morphology and the signature of the host galaxy.

♠ *ugriz* comparative analyses by magnitude and redshift classes

♠ forthcoming observation campaigns: NOT and CFHT

2) Astrometric and photometric variability.

♣ selected early results

♣ exponential model routines for photometric variability; implementation; and first results

3) Perspectives.

♥ QSO selection

♥ Core Catalog formation

1) <u>Morphology and the signature of the host galaxy</u>

♠ For AGNs in general, therefore also for QSOs, the host galaxy absolute magnitude should be brighter than -23.5.

♠ The host galaxy is thought of most of times be an elliptical or bulge dominated galaxy.

♠ The host galaxy luminosity seems to increase proportionally to the strength of the central source, i.e. QSOs host galaxies may expected to usually be brighter than those around less powerful AGNs.

♠ The size of the host galaxy also tends to follow the rule. Typical sizes for BLLac are 13kpc.

♠ Host galaxies have regularly been resolved for AGNs to z < 1.5 and 1arcsec resolution. Less regularly so for QSOs.

♠ The QSO space distribution peaks at z=0.6 for B=19, and at z=1 for for B=20.

♠ That is, the largest fraction of GAIA QSOs would be of nearby ones.

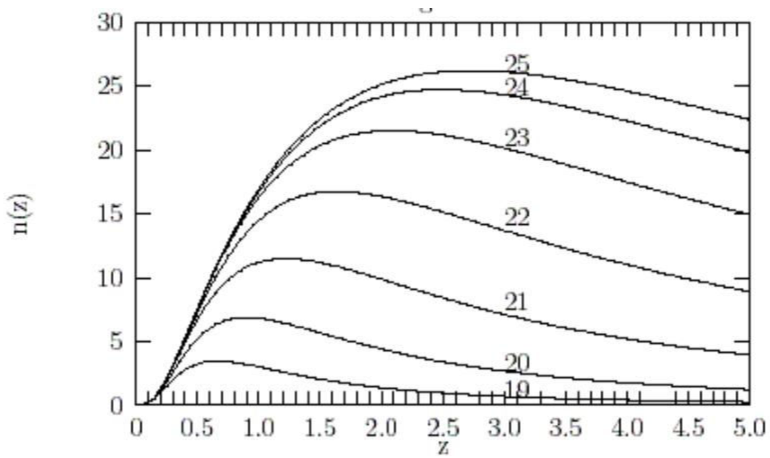

Number of quasars per deg^2 as function of redshift and magnitude (Crawford 1994)

1) Morphology and the signature of the host galaxy

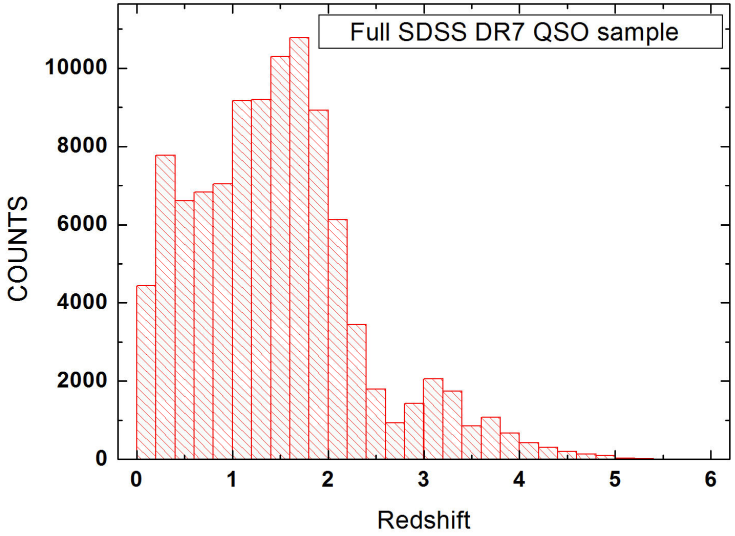

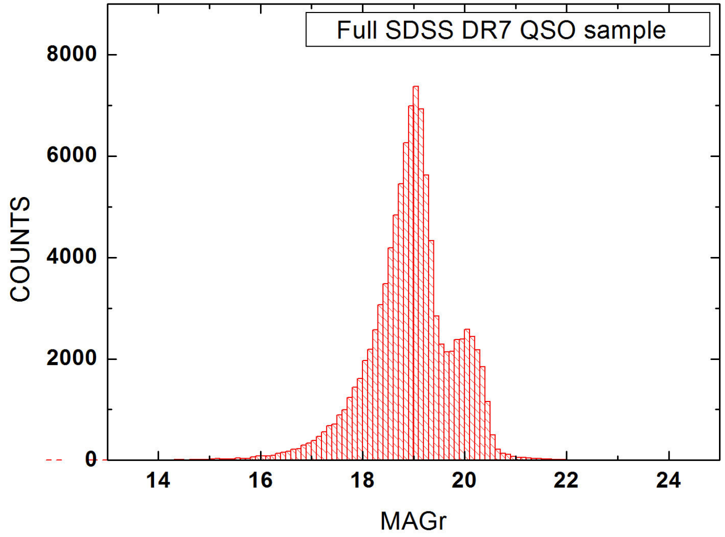

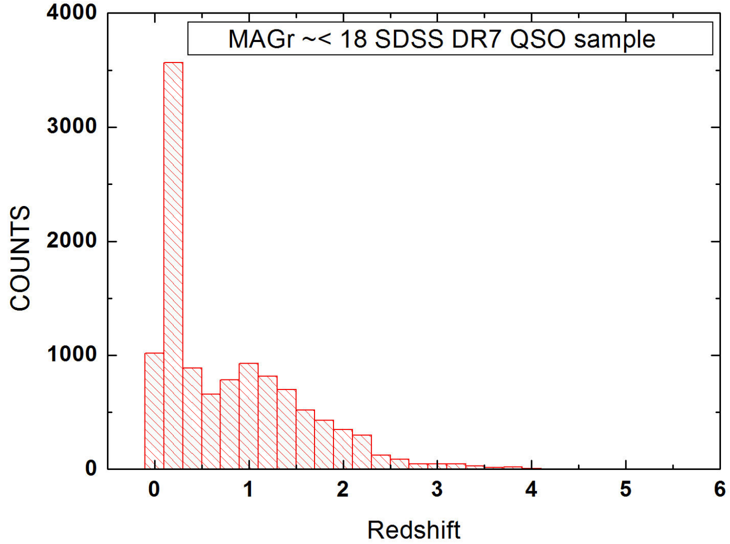

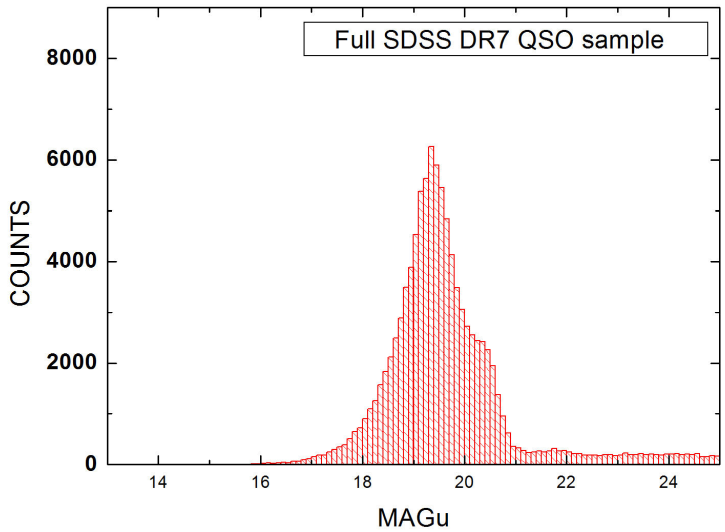

- The largest fraction of GAIA QSOs would be of nearby ones.
- Average z = 1.18 ; but z = 0.8 at MAGr ~<18

1) Morphology and the signature of the host galaxy

♠ Extracted 2048 × 1489 pixels (at 0”.396 arcsec/pixel → 13’.5 sec δ × 9”.8) regions containing the 105,783 spectroscopically confirmed QSOs in the latest catalog of the SDSS (2010) for the five *ugriz* colors.

♠ each frame is 3 – 4 Mb, totaling 1.5 – 2 Tb

Same QSO in more than one frame

Color	*u*	*g*	*r*	*i*	*z*
Number	1,355	628	2,286	1,983	263
σ SHARP	1.8	1.2	1.0	1.7	2.1
Range SHARP	15.9	12.4	12.6	18.3	21.4
σ SROUND	1.4	1.2	0.9	1.5	1.9
Range SROUND	12.2	14.1	15.9	14.0	14.0
σ GROUND	1.2	1.1	0.8	1.6	1.9
Range GROUND	14.4	16.8	18.4	30.6	16.7

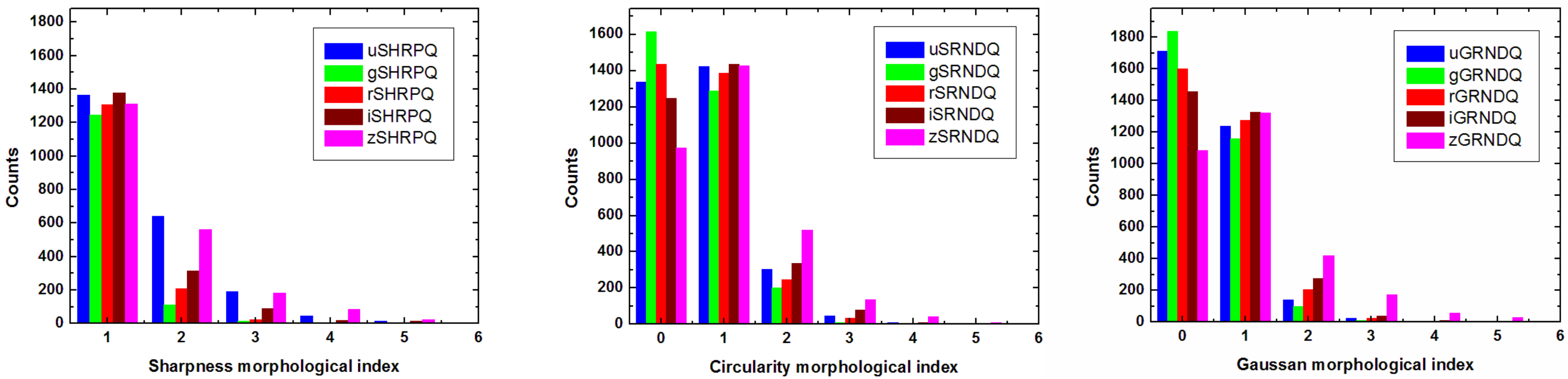

1) Morphology and the signature of the host galaxy

♠ **SDSS *r* magnitude** Morphological indexes IRAF's SHARP, SROUND, and GROUND, calculated by comparing the QSO's PSF against the mean surrounding PSF.

♠ Each point is the average for 10 objects randomly chosen to represent the class

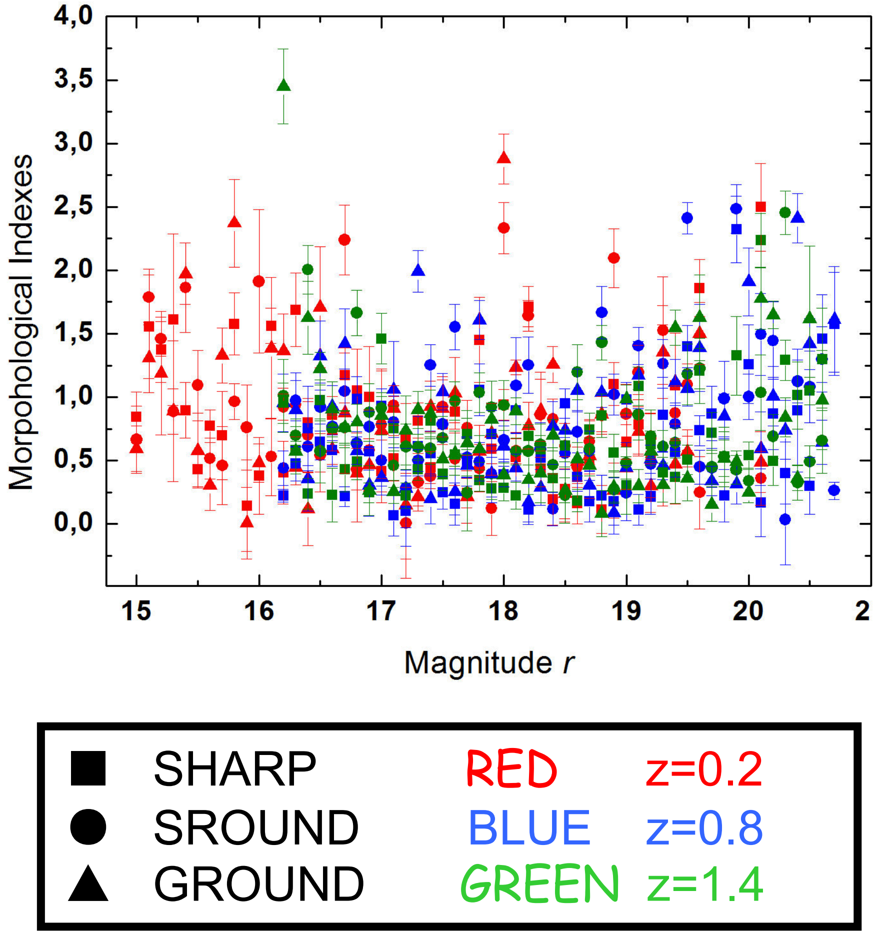

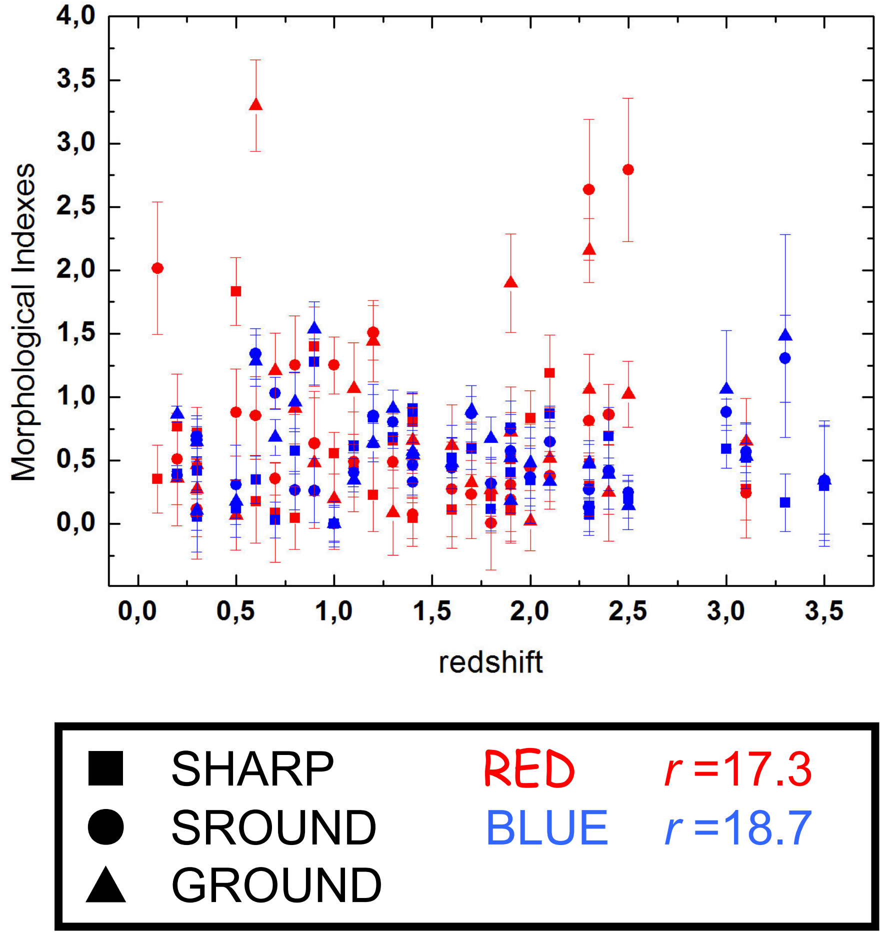

1) Morphology and the signature of the host galaxy

♠ **SDSS *u* magnitude** Morphological indexes IRAF's SHARP, SROUND, and GROUND, calculated by comparing the QSO's PSF against the mean surrounding PSF.

♠ Each point is the average for 10 objects randomly chosen to represent the class

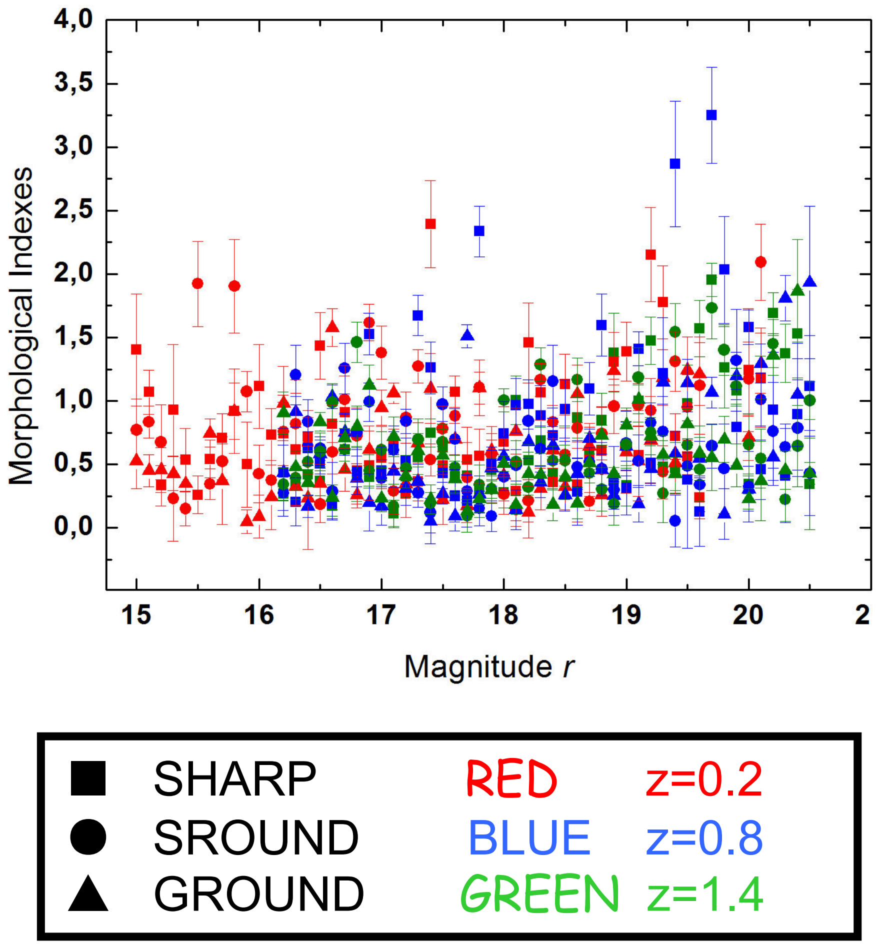

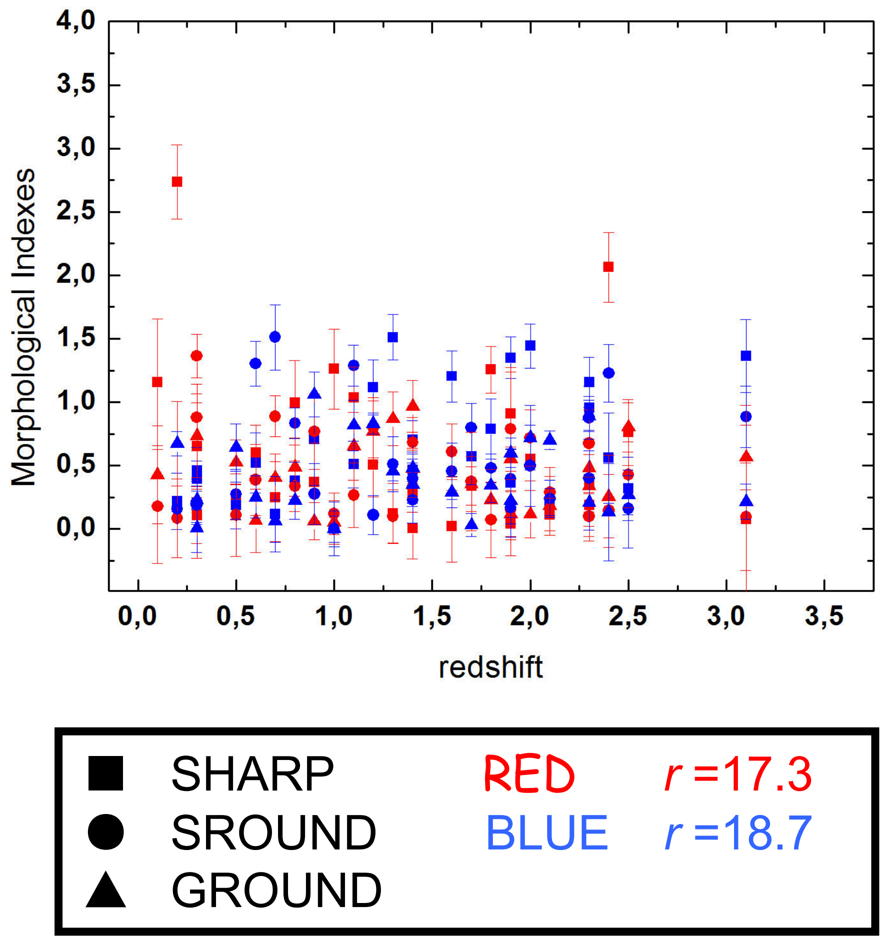

1) <u>Morphology and the signature of the host galaxy</u>

♠ **SDSS *i* magnitude** Morphological indexes IRAF's SHARP, SROUND, and GROUND, calculated by comparing the QSO's PSF against the mean surrounding PSF.

♠ Each point is the average for 10 objects randomly chosen to represent the class

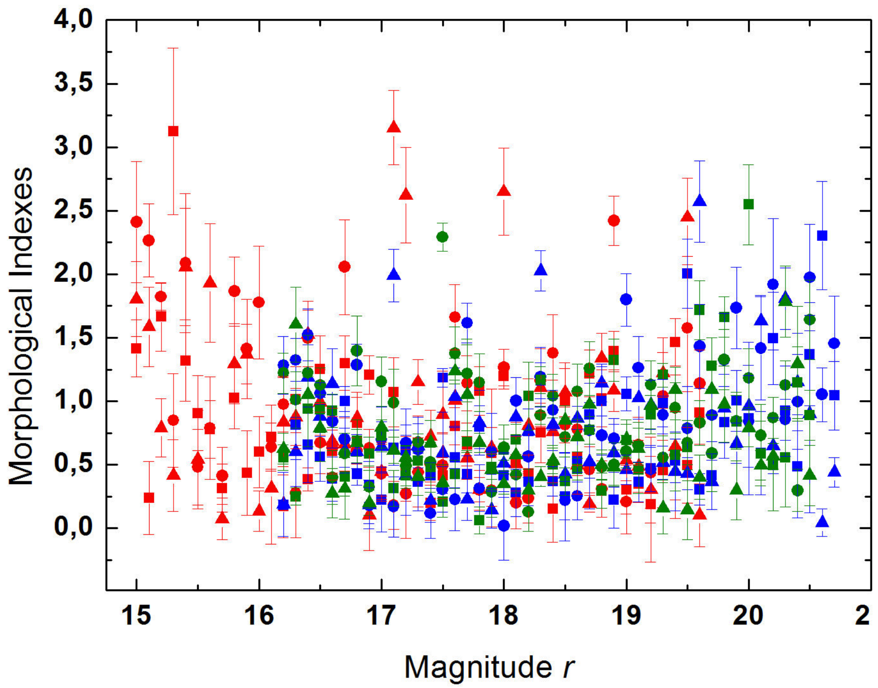

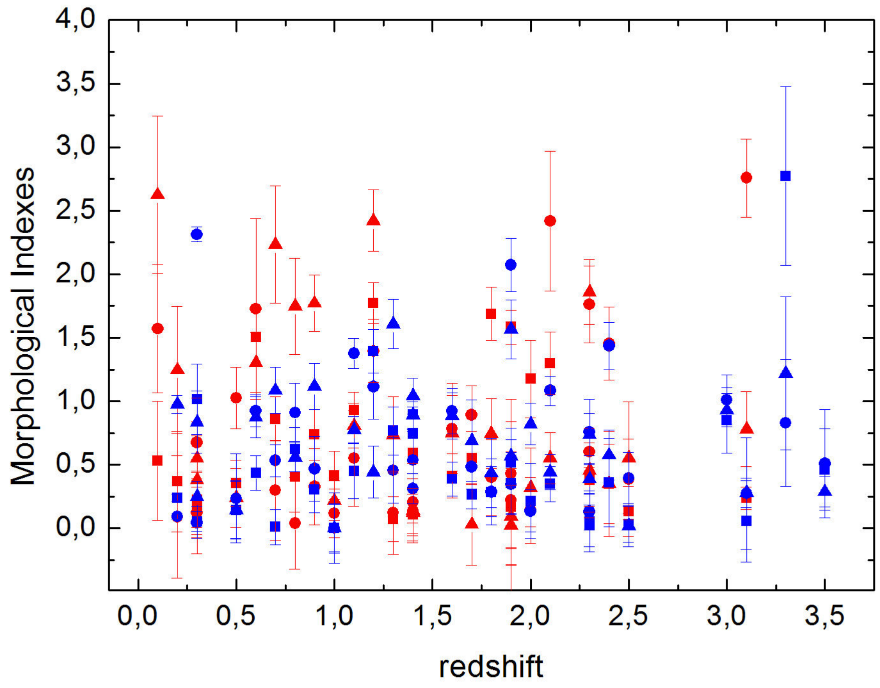

■	SHARP	RED	z=0.2
●	SROUND	BLUE	z=0.8
▲	GROUND	GREEN	z=1.4

■	SHARP	RED	*r* =17.3
●	SROUND	BLUE	*r* =18.7
▲	GROUND		

1) Morphology and the signature of the host galaxy and beyond

♠ 2012/2013 dedicated observing time.

♠ Nordic Optical Telescope – 2.5m telescope at the Canarias, Spain; 1024 × 1024 NOTcam CCD to 0".234/px and high resolution to 0".078/px.

♠Time awarded for high SNR photometry and morphology observation of QSRs for the Gaia to ICRFn link.

♠CFHT – 4m telescope at Hawaii; MEGACAM detector 1deg × 1deg field to 0".187/px.

♠ Same program as above - high SNR photometry and morphology observation of QSRs for the Gaia to ICRFn link – but with up to 49 comparison QSOs in each field.

- Mapping by **reverberation** measures the size of the broad emission-line region and size (hence the mass) of the central black hole in AGNs.
- ADS NASA list 989 papers on the subject in the last year only (e.g., Torino group monitoring, Lick project, etc).
- Pushkarev et al (2012 A&A, to appear) investigated a frequency-dependent shift in the absolute position of the optically thick apparent origin of parsec-scale jets of 163 sources. Found median values of 128,125, and 88 μas, for Δv from 8 to 3GHz.

2) Astrometric and photometric variability

♣ One of the most important constraints on the structure of quasars is variability. It must assuredly be linked to some degree of motion of the photocenter. The demands of accuracy for the objects forming the fundamental astrometric frame of GAIA make mandatory a larger comprehension about the astrometric wandering of the photocenter and ìndeed a deeper comprehension of the mechanisms giving rise to optical emission in quasars.

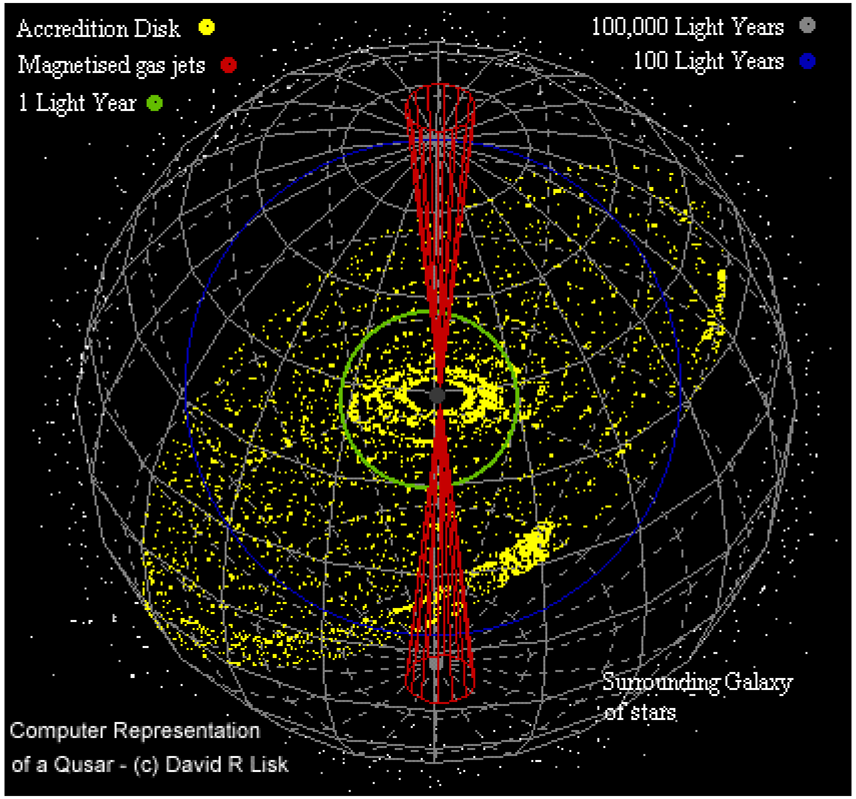

♣ Since long, year/month-like, and large amplitude variations are also recorded, the sstandard reasoning itself would suggest that the other quasar's elements aren't at a stand-still.

♣ There are several mechanisms apt to generate the optical and positional variability. **Opacity changes off the core regions; instabilities propagated from the accretion disk; emission from a precessing/disturbed jet; v ariability powered by a series of supernovae explosions; conversely variability triggered by stellar masses plunged towards the accretion disk; emission from regions at superluminal speeds; luminosity disturbance brought by the host galaxy; microlensing.**

2) <u>Astrometric and photometric variability</u>

♣ Share the same field of view and primary mirrors.

♣ The preceding and following astrometric fields of view (i.e., separated by an angle of 106 deg) have a repetition observing pattern of: 1h46m-4h14m-1h46m-4h14m.

♣ Typically, the objects are observed during 4-5 orbits and then gaps of about 30-40 days will separate these grouped measurements (depending of the object position).

♣ When an object is temporarily at the node of the great circle of scanning, it is regularly observed for several days.

♣ Raw centroids are sensitive to chromatic aberrations to several mas, that will be corrected through the onboard photometric mea surement.

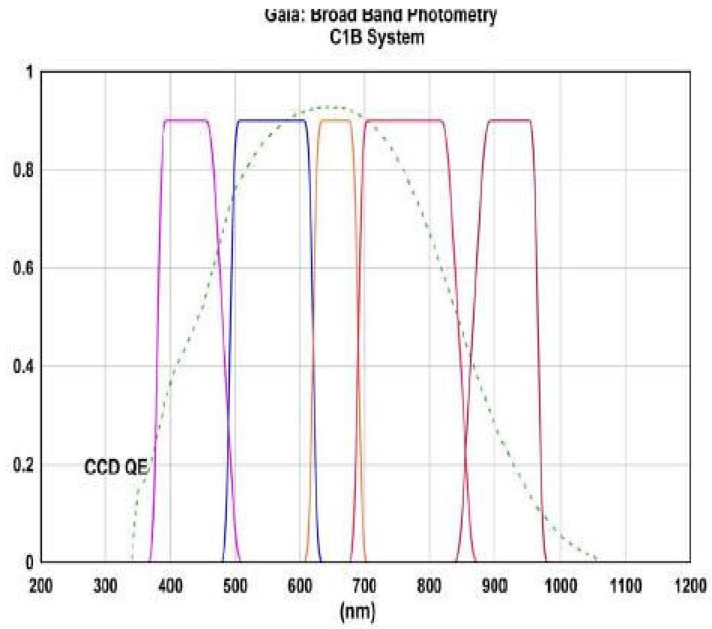

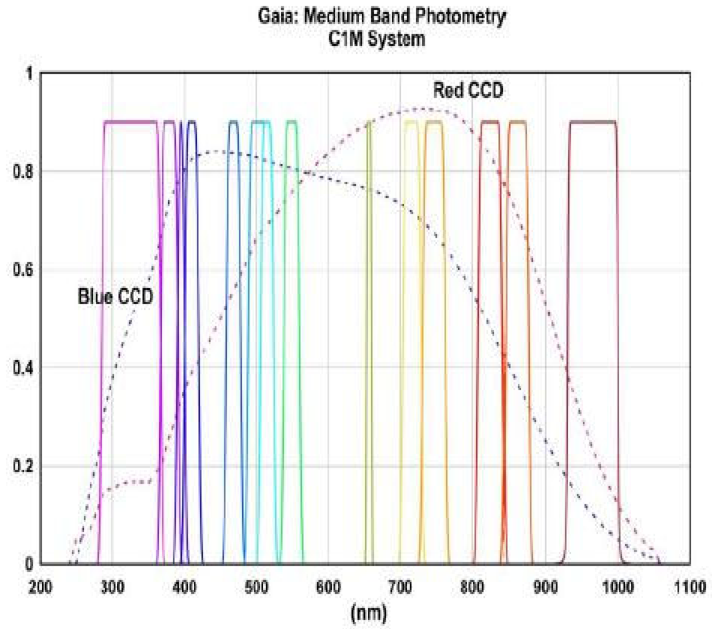

2) <u>Astrometric and photometric variability</u>

r X10 for QSOs !

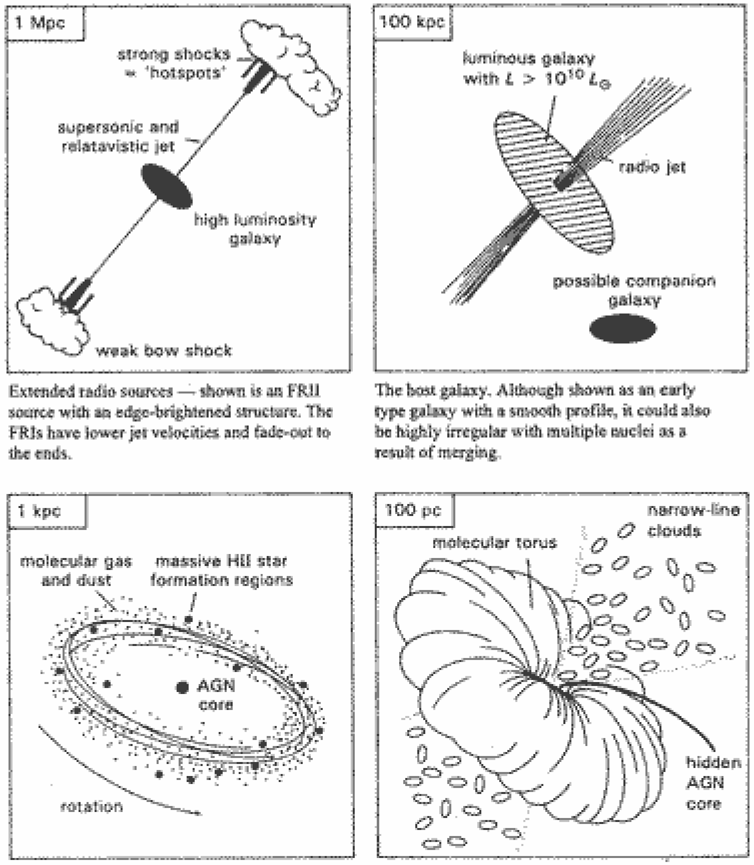

Extended radio sources — shown is an FRII source with an edge-brightened structure. The FRIs have lower jet velocities and fade-out to the ends.

The host galaxy. Although shown as an early type galaxy with a smooth profile, it could also be highly irregular with multiple nuclei as a result of merging.

The central kpc star formation disk. This strong far infrared emitting zone might be fed by a bar structure, as seems to be the case for NGC1068.

The narrow-line region comprising small but numerous clouds of the interstellar medium ionized by the central AGN core.

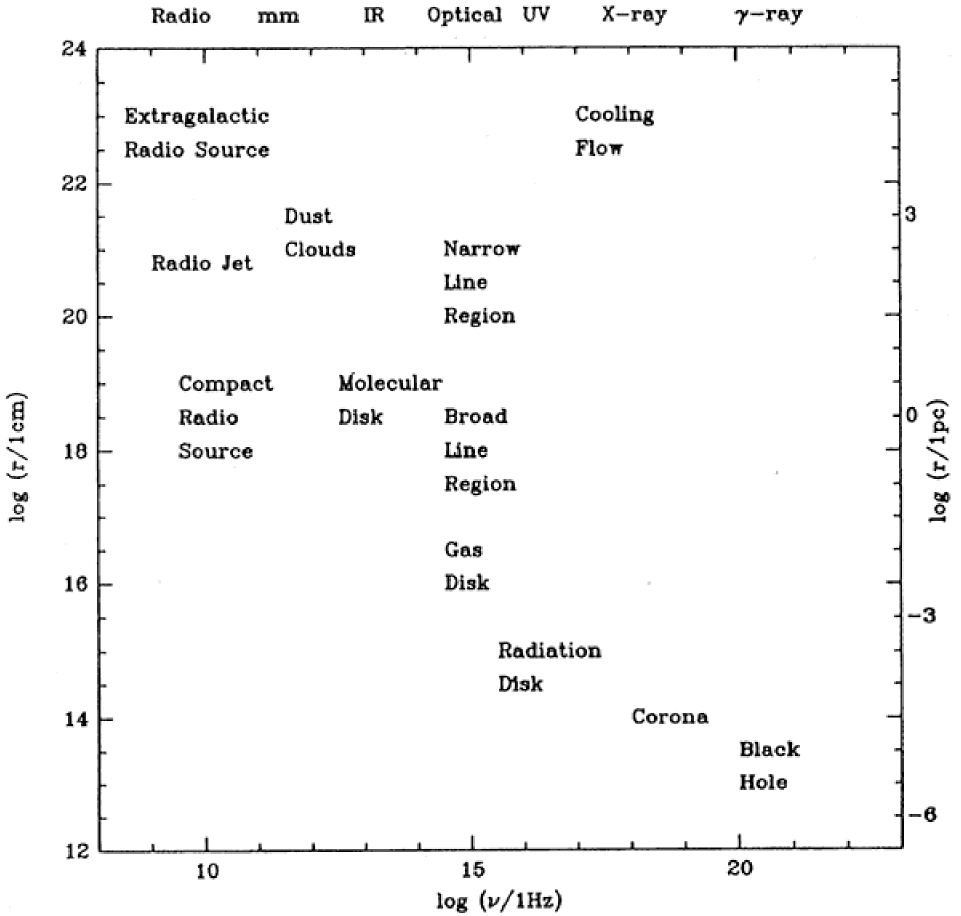

Fig. 1.1. Schematic illustration of the range of activity associated with the nuclei of galaxies. Phenomena have been observed spanning the full dynamic range of $\sim$ 45 octaves of length scale from variable X-ray emission in Seyferts ($\lesssim 10^{12}$cm) to giant double radio sources ($\gtrsim 10^{25}$cm) and from metre wavelengths (low frequency variability) to 100MeV observations of some quasars and Seyfert galaxies (45 octaves of frequency). Some of these phenomena, *e.g.* radio jets, are observed directly. Others, *e.g.* accretion disk coronae and black holes are inferred indirectly and are of more questionable reality.

(*credit Bradford's SAAS Fee 1990 lectures*)

2) Astrometric and photometric variability

♣ ESO Max Planck 2.2m telescope, La Silla, Chile, 0".238/pixel, WFI nearby the optical axis. Filters Rc/162 (peak 651.7nm, FWHM 162.2nm) and BB#B/123 (peak 451.1nm, FWHM 135.5nm). In each filter 3 frames are taken, to a combined SNR of 1000 (up to 2h total integration time).

♣ Relative astrometry (1mas) and

photometry (0.001mag)

$$C_n^m - \langle C \rangle_n^m = C_0 + \sum_{i,j,k}^{1,3} A_{ijk} X^i Y^j M^k$$

♣ Linear Pearson correlation and Non-parametric Spearman correlation (statistical error in brackets).

QSO	ΔX /ΔMag		ΔY /ΔMag		JitterX/ ΔMag		JitterY/ ΔMag	
	Pearson	Spearman	Pearson	Spearman	Pearson	Spearman	Pearson	Spearman
1512-0905	-0.42 (0.59)	-0.49 (0.33)	0.85 (0.00)	0.77 (0.33)	-0.80 (0.43)	-0.94 (0.00)	0.79 (0.00)	0.89 (0.02)
1620+1724	0.94 (0.00)	0.90 (0.04)	0.81 (0.01)	0.80 (0.10)	0.31 (0.48)	0.00 (1.00)	-0.30 (0.71)	-0.60 (0.28)
1620+1736	0.14 (0.76)	0.03 (0.96)	-0.52 (0.53)	0.09 (0.87)	0.38 (0.29)	0.31 (0.54)	-0.75 (0.44)	-0.49 (0.33)
1751+0939	0.58 (0.41)	0.50 (0.67)	-0.83 (0.73)	-0.50 (0.67)	0.96 (0.02)	1.00 (0.00)	0.62 (0.35)	0.50 (0.67)
0522-6107	0.44 (0.14)	0.46 (0.29)	-0.31 (0.62)	-0.32 (0.48)	0.22 (0.55)	0.36 (0.43)	0.15 (0.70)	0.14 (0.76)
0407-1211	-0.03 (0.97)	0.00 (1.00)	-0.12 (0.89)	-0.41 (0.60)	0.64 (0.13)	0.40 (0.60)	0.66 (0.11)	0.80 (0.20)
0442-0017	-0.46 (0.70)	-0.41 (0.60)	-0.40 (0.73)	-0.40 (0.60)	0.04 (0.96)	-0.80 (0.20)	0.40 (0.45)	0.40 (0.60)
0858+1651	-0.74 (0.61)	-0.20 (0.80)	-0.10 (0.91)	-0.20 (0.80)	-0.73 (0.61)	-0.20 (0.80)	-0.57 (0.66)	-0.80 (0.20)
1218+0200	0.03 (0.97)	0.20 (0.75)	-0.42 (0.64)	-0.50 (0.39)	-0.52 (0.59)	-0.70 (0.19)	-0.41 (0.65)	-0.30 (0.62)

Teerkopi (2003) QSOs selected for high amplitude, long term variability. This time-line 2.25y, at every 2-3 months, i.e. 5-8 runs/source.

2) Astrometric and photometric variability

♣ **Time line - up to 435 days. There was always a preferred direction of the jitter. For 1512-0905 and 0522-6107 the preferred direction changed on time – but keeping strong autocorrelation. Nearby stars do not show such autocorrelation**

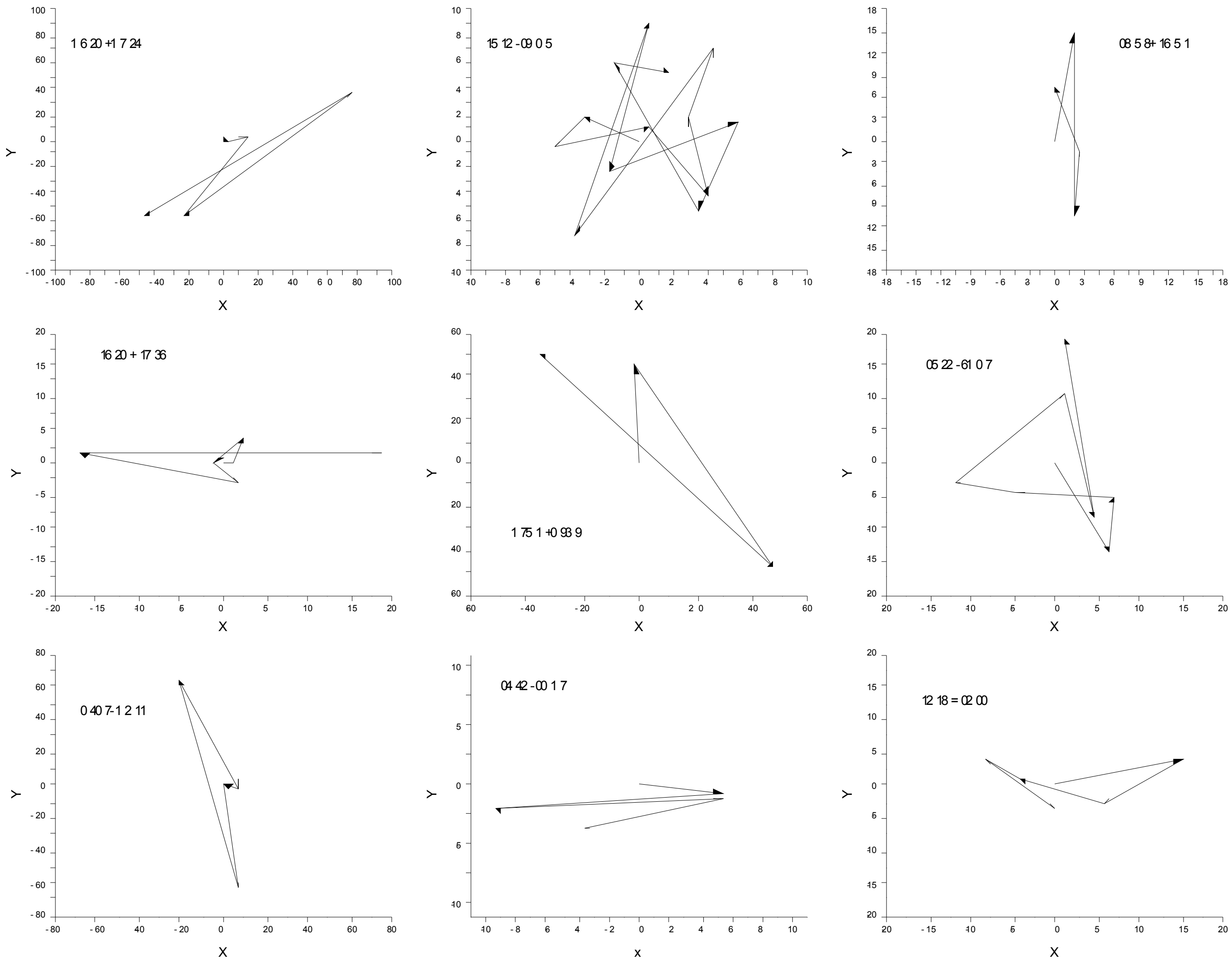

2) Astrometric and photometric variability

♣ 41 QSOs of the Deep 2 field were analyzed. QSOs images obtained during 4.5 years with the Canada France Hawaii Telescope (CFHT) in the frame of the CFHTLegacy Survey (CFHT-LS). All quasars showed variability, but the evidence of correlation is weak due the use of absolute astrometry.

♣ Relative PSF astrometry and photometry in the case of a QSO with a nearby star, evidentiates the correlation.

♣ CFHT image of the QSO 39436 with the nearby star (5” south). Correlation between the photocenter walk (green line) and the Blue and red magnitudes variation.

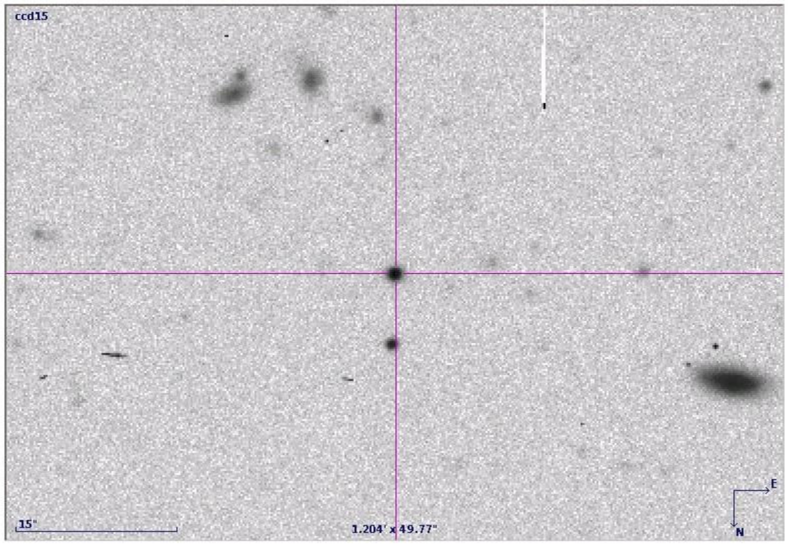

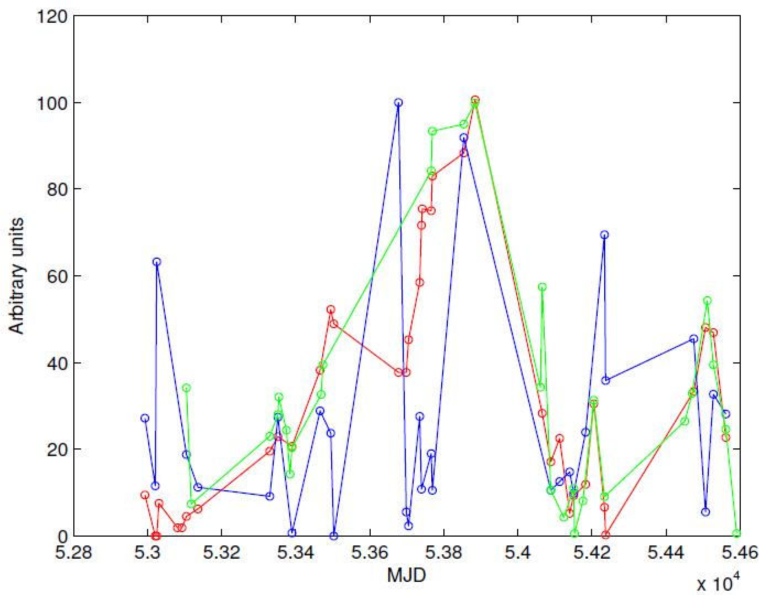

2) Astrometric and photometric variability

♣ G and R magnitude variation from the Zadko telescope – QSO 0007+106

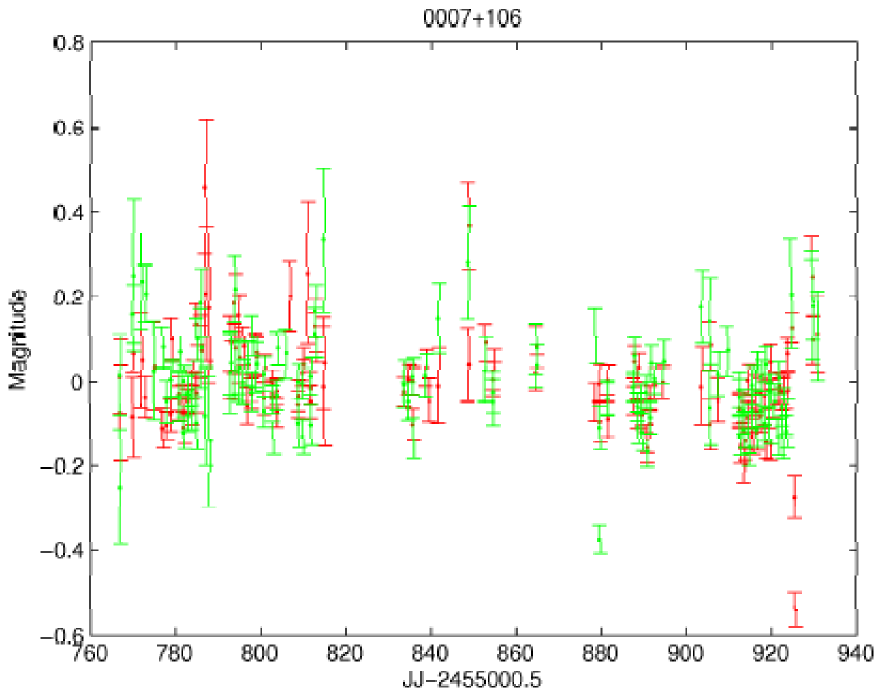

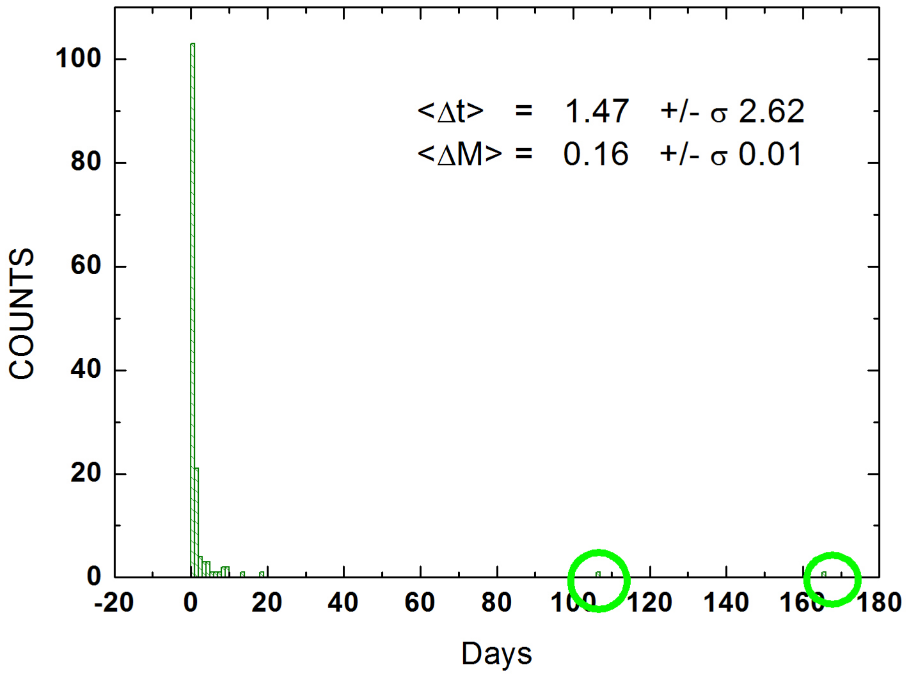

$A = 0.348 \pm 0.006$

$\gamma = 0.484 \pm 0.0009$

2) Astrometric and photometric variability

♣ G and R magnitude variation from the Zadko telescope – QSO 0109+224

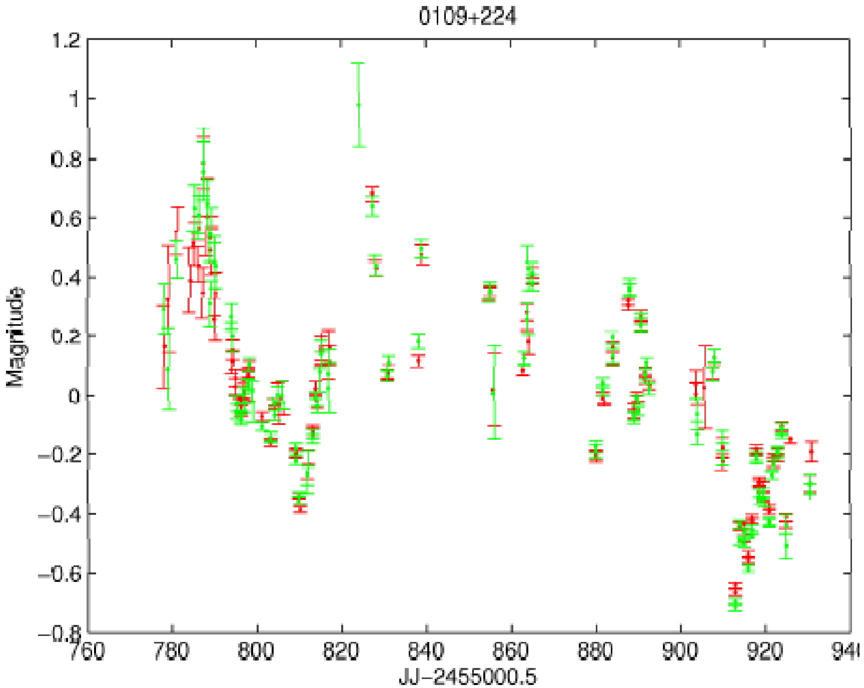

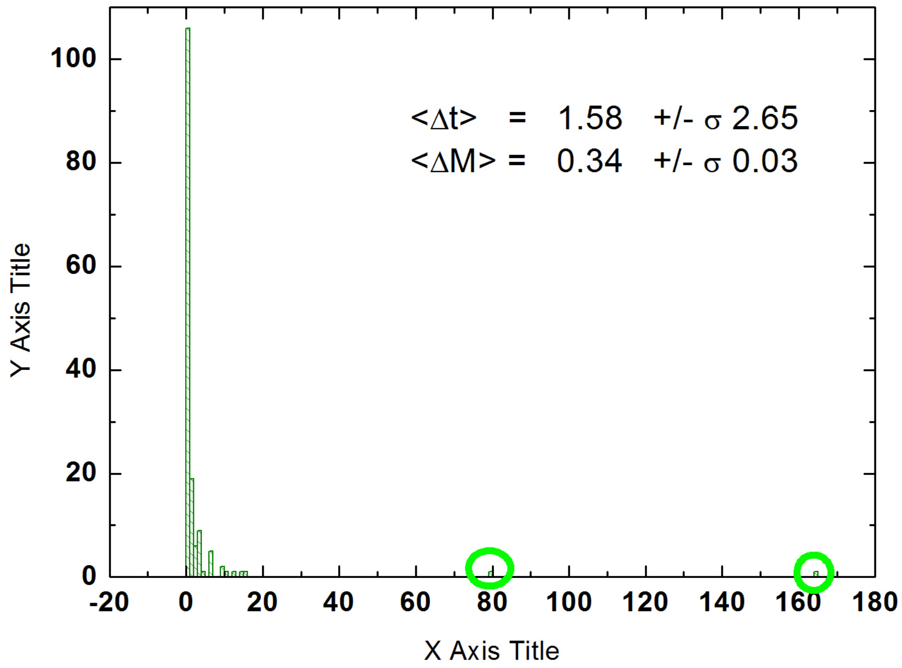

$A = 0.394 \pm 0.003$

$\gamma = 0.558 \pm 0.0003$

2) Astrometric and photometric variability

♣ G and R magnitude variation from the Zadko telescope – QSO 0716+714

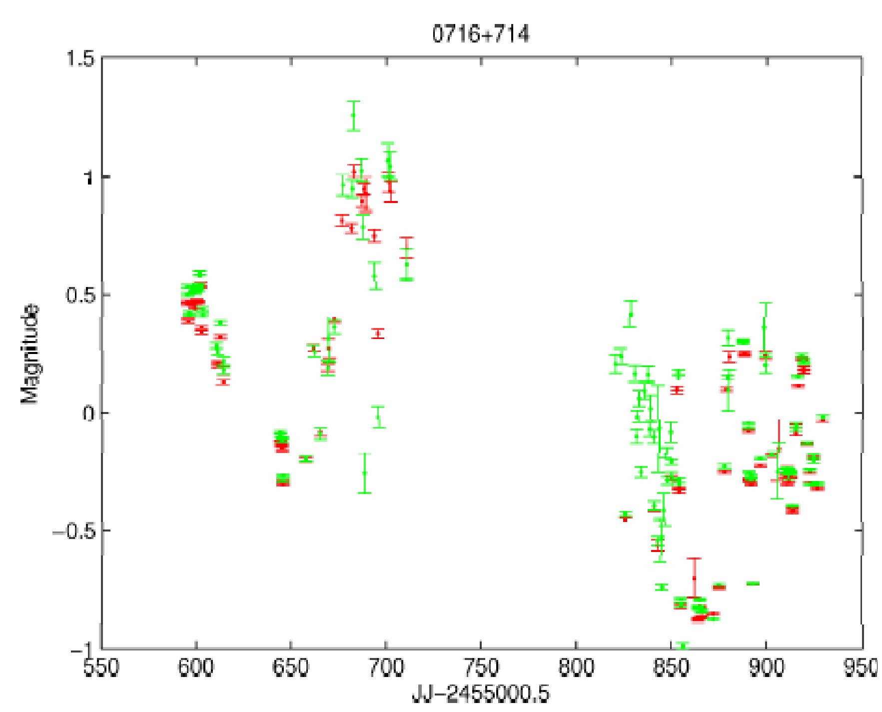

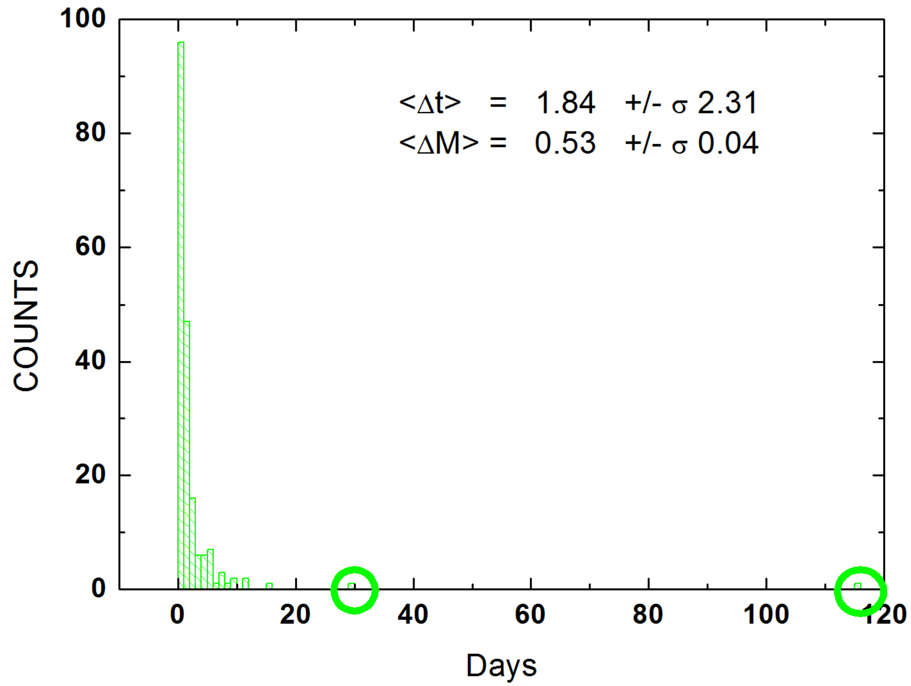

$A = 0.390 \pm 0.003$

$\gamma = 0.613 \pm 0.0005$

3) Perspetives

1) For the brightest (Gr 18th mag) QSOs the host galaxy isophotes might be present for about 20% of the objects. This does not hamper top astrometric precision if accounted for.

2) QSOs are inherently variable objects. This might hamper top astrometric accuracy if not accounted for.

3) Both morphology and optical variability can bring auxiliary means for QSOs onboard recognition. Much specially to disentangle from the color/magnitude stellar contaminants.

4) What is required for both morphology and variability analysis is already present in the Gaia observation. It is a matter of setting the analyzing methods and force tasks.

5) EO analysis might get results more comprehensive and effective by combining both morphology and variability (and astrophysical modeling) into a common database along the whole mission.

6) **Thank You. Questions? Comments?**